hydrogen atoms while maintaining the bond and dihedral angles, but shortening the bond lengths to 1.10 Å. The coordinates of this trimethylene were then submitted to Gaussian 90 for single-point calculations using the D95V basis set (Dunning's basis set). The GVB(1/2) singlet energy was −116.955 578 9 hartrees, and the ROHF triplet energy was −116.953 473 4 hartrees, indicating a singlet ground state and a singlet–triplet gap of 1.3 kcal/mol.

Matched OD Photolysis of 4-$(N_2)_2$ and 31. MTHF solutions of 4-$(N_2)_2$ with A(342 nm) = 1.4 and 31 with A(342 nm) = 1.3 were prepared. The solutions were pipetted into quartz EPR tubes fitted with vacuum stopcocks and submitted to five freeze–pump–thaw cycles. Samples were irradiated sequentially at 50 K using the same source and filter combination. Plots of signal intensity vs photolysis time are shown in Figure 7.

Variable-Temperature EPR Study of 3. An EPR sample of 3-$(N_2)_2$ in 1,2-propanediol was photolyzed for 6 h at 50 K. The temperature was raised briefly (~5 min) to 120 K in order to anneal the sample, and spectra were taken at decreasing temperatures down to 10 K.

Simulation of EPR Spectra. We modified a published procedure[26] for the computation of EPR powder spectra. The EPR spin Hamiltonian used is shown in eq 6, shown again here for convenience.

$$\hat{H} = g\beta \mathrm{B}\cdot\hat{S} + D(\hat{S}_z{}^2 - (S(S+1)/3)) + E(\hat{S}_x{}^2 - \hat{S}_y{}^2) \quad (6)$$

The expression for the first-derivative powder spectrum is[26,36,37]

$$\frac{\partial I}{\partial B} = \sum_{i<j}\int_0^{\pi/2}\int_0^{\pi/2}\langle V_{ij}\rangle\frac{\partial B}{\partial v}\frac{\partial}{\partial B}\left(\frac{1}{(2\pi)^{1/2}\sigma_{ij}}e^{-1/2[((B-B_0)/\sigma_{ij}]^2}\right)\sin\theta\,d\theta\,d\phi \quad (13)$$

Numerical integration of eq 13 was required in order to simulate spectra. Parameters θ and ϕ were varied in 1° increments between 0° and 90°. At each orientation, the resonant fields for each of the $\Delta m_s = 1$ and $\Delta m_s = 2$ transitions were computed by solving the resonance condition $E_i - E_j = g\beta B$ by interative diagonalization of the Hamiltonian matrix of eq 1. Once the resonance field was found for a given transition, the eigenvectors $|i\rangle$ and $|j\rangle$ belonging to the two energy eigenvalues E_i and E_j were computed as linear combinations of the $\hat{S}_z$ basis functions. The transition probability could then be calculated according to eq 14.[26,37,38] The

$$\langle V_{ij}\rangle = \frac{\pi g^2\beta^2 B_1}{2}\left[\left|\langle i|\cos\theta\cos\phi\,\hat{S}_x + \cos\theta\sin\phi\,\hat{S}_y + \sin\theta\,\hat{S}_z|j\rangle\right|^2 + |\langle i\sin\phi\,\hat{S}_x - \cos\phi\,\hat{S}_y|j\rangle|^2\right] \quad (14)$$

derivative $\partial B/\partial v$ was approximated as $h/g\beta\Delta m_s$.[36,39] Powder spectra were obtained in final form by fitting a Gaussian line shape to the single transitions computed above and summing over all transitions. Line widths in powder EPR spectra are orientation-dependent; thus the line width was represented as a diagonal tensor σ.[26,38,39] The width of the Gaussian applied to a given transition was determined from eq 15.[26]

$$\sigma_{ij}^2 = (\cos\theta\cos\phi\,\sigma_{x_{ij}})^2 + (\cos\theta\sin\phi\,\sigma_{y_{ij}})^2 + (\sin\theta\,\sigma_{z_{ij}})^2 \quad (15)$$

Acknowledgment. We thank Dr. Angelo J. Di Bilio for providing us a copy of his program for EPR simulation, and Dr. Di Bilio and Dr. Sunney I. Chan for fruitful discussions of EPR results and spectral simulations. This work was funded by the National Science Foundation, to whom we are grateful.

---

(36) Aasa, R.; Vänngård, T. *J. Mag. Res.* **1975**, *19*, 308.
(37) van Veen, G. *J. Magn. Reson.* **1978**, *91*, 30.
(38) Wasserman, E.; Snyder, L. C., Yager, W. A. *J. Chem. Phys.* **1964**, *41*, 1763.
(39) Koitis, P.; Lefebvre, R. *J. Chem. Phys.* **1964**, *41*, 379.

Molecular Solid-State Organometallic Chemistry of Tripodal (Polyphosphine)metal Complexes. Catalytic Hydrogenation of Ethylene at Iridium

Claudio Bianchini,*,† Erica Farnetti,‡ Mauro Graziani,*,‡ Jan Kaspar,‡ and Francesco Vizza†

Contribution from the Istituto per lo Studio della Stereochimica ed Energetica dei Composti di Coordinazione, CNR, Via J. Nardi 39, 50132 Firenze, Italy, and Dipartimento di Scienze Chimiche, Università di Trieste, Via Valerio 38, 34127 Trieste, Italy. *Received March 27, 1992*

Abstract: The solid–gas reactions of [(triphos)Ir$(H)_2(C_2H_4)$]BPh_4 (1) with CO, C_2H_4, and H_2 are described [triphos = $MeC(CH_2PPh_2)_3$]. The gaseous reactants promote the elimination of ethane from 1 and the formation of [(triphos)Ir$(CO)_2$]BPh_4, [(triphos)Ir$(C_2H_4)_2$]BPh_4, and [(triphos)Ir$(H)_2$]BPh_4, respectively. The latter 16-electron species is isolable in the solid state at temperatures <70 °C. At higher temperatures, [(triphos)Ir$(H)_2$]$^+$ dimerizes in the solid state to give the tetrahydride [(triphos)HIr$(\mu\text{-}H)_2$HIr(triphos)]$^{2+}$. Dimerization is avoided when the unsaturated fragment is incorporated into the lattice of a polyoxometalate cluster such as $PW_{12}O_{40}{}^{3-}$. The complex [(triphos)Ir$(H)_2(C_2H_4)$]BPh_4 is an effective catalyst for the hydrogenation of ethylene in the solid state at 60 °C. Comparisons are made with analogous fluid solution-phase systems.

Molecular solid-state organometallic chemistry is experiencing rapid growth through the reactions of materials derived from either metal oxide clusters of the Keggin-ion type[1] or tripodal polyphosphine ligands.[2]

We are developing the solid-state chemistry of Group VIII metal complexes stabilized by tripodal polyphosphines such as $P(CH_2CH_2PPh_2)_3$ (PP$_3$), $N(CH_2CH_2PPh_2)_3$ (NP$_3$), and $MeC(CH_2PPh_2)_3$ (triphos) (Scheme I).

Scheme I

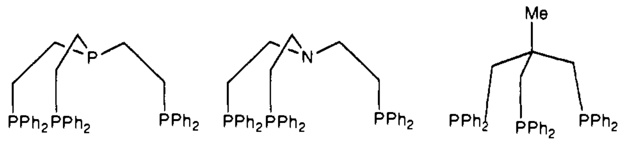

PP$_3$ NP$_3$ lriphos

Earlier work has shown that (i) the Co(I) complex [(PP$_3$)Co(N_2)]BPh_4 (1) reacts in the solid state with a variety of gaseous

---

† CNR, Florence.
‡ University of Trieste.

0002-7863/93/1515-1753$04.00/0

Scheme II. Solution Chemistry of **1**

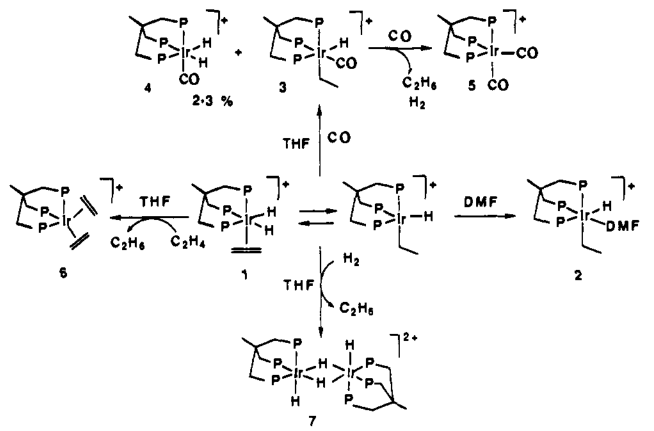

molecules to form either 1:1 adducts ($H_2C{=}CH_2$, CO, H_2) or products derived from C—H bond activation at cobalt ($HC{\equiv}CH$, CH_2O, MeCHO)[2a,c] and (ii) the *cis*-hydride alkynyls $[(PP_3)Co(H)(C{\equiv}CR)]BPh_4$ thermally rearrange to the corresponding vinylidenes $[(PP_3)Co\{C{=}C(H)R\}]BPh_4$ in the solid state (R = H, Ph, *n*-C_3H_7, *n*-C_5H_{11}, CMe_3, $SiMe_3$).[2b]

It is believed that (i) small organic molecules can penetrate the crystal of the tetraphenylborate salts of tripodal(polyphosphine)metal complexes, dissolving in the extensive hydrophobic region comprised of as many as ten phenyl rings and six methylenic chains per molecule and (ii) facile access to each metal center in the crystal lattice is provided at relatively high temperatures by the motional freedom of the phosphine arms of the tripodal ligands.

This paper describes the first examples of stoichiometric and catalytic solid–gas reactions assisted by the tripodal triphosphine triphos. The ligand triphos is known to form very stable complexes with most d-block metals in a variety of stereochemistries.[3] In all cases, however, triphos occupies three facial sites on the coordination polyhedra, thus leaving as many as three free sites at the metal center. Therefore, as compared to PP_3, triphos metal fragments favor multistep reaction sequences such as olefin-based reactions. Indeed, several triphos complexes, particularly those with Ir and Rh, have been found to act as effective homogeneous catalysts for hydroformylation,[4] hydrogenation,[4-6] isomerization,[5,6] oligomerization,[7] amination, and related nucleophilic additions to olefins.[8]

In the present paper, we report on the ability of the *cis*-dihydride ethylene complex $[(triphos)Ir(H)_2(C_2H_4)]BPh_4$[8] (**1**) to activate *in the solid state* important reactive ligands such as ethylene, dihydrogen, and carbon monoxide. In particular, the reactivity of **1** as catalyst for the solid–gas hydrogenation of ethylene will be compared with that in analogous fluid solution-phase systems.

As will be apparent in forthcoming pages, (triphos)metal moieties possess the potential requisite to become ideal systems for study at the molecular level of the mechanism of many heterogeneous organometallic reactions.

Results and Discussion

Solution Chemistry of $[(triphos)Ir(H)_2(C_2H_4)]BPh_4$. For a better understanding of the solid–gas reactions described in this paper, it is worth recalling some aspects of the solution chemistry of **1** (Scheme II).[8]

In poorly coordinating solvents (CH_2Cl_2, $CHCl_3$, THF) at room temperature, the dihydride ethylene complex **1** is in a rapid equilibrium with its hydride-migration product $[(triphos)Ir(H)(C_2H_5)]^+$, which can be stabilized by donor solvents such as dimethylformamide (DMF) to give the octahedral adduct $[(triphos)Ir(H)(C_2H_5)(DMF)]^+$ (**2**).

The stabilization of the hydride ethyl form of **1** can be achieved also by reaction with CO (1 atm) in THF to give the hydride ethyl carbonyl $[(triphos)Ir(H)(C_2H_5)(CO)]^+$ (**3**), which transforms into the dicarbonyl $[(triphos)Ir(CO)_2]^+$ (**5**) upon treatment with further CO. During the course of the reaction, ethane is almost quantitatively eliminated. A small amount of the dihydride carbonyl complex $[(triphos)Ir(H)_2(CO)]^+$[9] (**4**) can eventually form by competitive elimination of C_2H_4 from **1**.

Compound **1** eliminates C_2H_6 also by reaction with ethylene (1 atm) to give the bis(ethylene) complex $[(triphos)Ir(C_2H_4)_2]^+$ (**6**). Finally, by treatment of **1** in THF with H_2 (1 atm) at reflux temperature, $[(triphos)IrH(\mu\text{-}H)_2HIr(triphos)]^{2+}$ (**7**) is quantitatively obtained. The tetrahydride **7** in THF solution reacts with neither C_2H_4 nor CO, even at high temperature.

All cations of Scheme II were employed as BPh_4^- salts.

Solid-State Chemistry of $[(triphos)Ir(H)_2(C_2H_4)]BPh_4$. Thermal Behavior under Inert Atmosphere. Compound **1** appears as off-white crystals, quite stable in the solid state under inert atmosphere (N_2, Ar, or He) or under reduced pressure (0.1 Torr) at 100 °C. Differential scanning calorimetry (DSC) shows no well-defined phase change up to 197 °C, at which temperature the compound begins to decompose. However, a continuous drift of the base line is observed above 110 °C which indicates a slow but effective thermal transformation occurring in the solid state. As a matter of fact, a temperature-programmed decomposition experiment (TPDE) carried out in a flow of helium (20 mL min^{-1}) at a heating rate of 5 °C/min up to 150 °C showed evolution of ethane and ethylene in ca. 4:1 ratio starting approximately at 110 °C (Scheme III).

Identification of the iridium products after the thermal decomposition reaction was made by IR (Nujol mulls, KBr) and NMR spectroscopy. The IR spectrum shows a significant change of the ν(Ir–H) stretching region, which now contains a broad absorption at 2123 cm^{-1} instead of the two bands at 2110 and 2062 cm^{-1} of the starting dihydride **1**.[8] Also, a band at 585 cm^{-1} typical of **1** has disappeared. Dissolution of the product in DMF-d_7 produces a colorless solution which can be analyzed by $^{31}P\{^1H\}$ NMR spectroscopy. The ^{31}P spectrum shows the solution to contain the tetrahydride **7** and undefined phosphorus-containing products (the largest signal falls at −25 ppm, where the resonance of free triphos is generally observed) in ca. 1:4 ratio (based on NMR integration). The evolution of C_2H_6 suggests that, like in solution, **1** may convert in the solid state to its hydride-migration product, which is appropriate to undergo the reductive elimination of ethane. Once ethane is liberated, the reduced $[triphos)Ir]^+$ system would not be sufficiently stable in the solid state, and thus it would decompose.

Interestingly, the presence of the tetrahydride **7** is found also when the crude product is dissolved in coordinating solvents such as DMF or THF saturated with CO. This finding is of particular

---

(1) (a) Siedle, A. R.; Newmark, R. A. *Organometallics* **1989**, *8*, 1442. (b) Siedle, A. R.; Newmark, R. A. *J. Am. Chem. Soc.* **1989**, *111*, 2058. (c) Siedle, A. R.; Newmark, R. A.; Sahyun, M. R. V.; Lyon, P. A.; Hunt, S. L.; Skarjune, R. P. *J. Am. Chem. Soc.* **1989**, *111*, 8346. (d) Siedle, A. R.; Lyon, P. A.; Hunt, S. L.; Skarjune, R. P. *J. Am. Chem. Soc.* **1986**, *108*, 6430.

(2) (a) Bianchini, C.; Peruzzini, M.; Zanobini, F. *Organometallics* **1991**, *10*, 3415. (b) Bianchini, C.; Peruzzini, M.; Vacca, A.; Zanobini, F. *Organometallics* **1991**, *10*, 3698. (c) Bianchini, C.; Mealli, C.; Peruzzini, M.; Zanobini, F. *J. Am. Chem. Soc.* **1992**, *114*, 5905.

(3) (a) Sacconi, L.; Mani, F. *Transition Met. Chem.* (N.Y.) **1982**, *8*, 179. (b) Bianchini, C.; Mealli, C.; Meli, A.; Sabat, M. In *Stereochemistry of Organometallic and Inorganic Compounds*; Bernal, I., Ed.; Elsevier: Amsterdam, 1986; Vol. 1, p 146. (c) Bianchini, C. *Comments Inorg. Chem.* **1988**, *8*, 27.

(4) Bianchini, C.; Meli, A.; Peruzzini, M.; Vizza, F.; Frediani, P.; Ramirez, J. A. *Organometallics* **1990**, *9*, 226 and references therein.

(5) Bianchini, C.; Meli, A.; Laschi, F.; Ramirez, J. A.; Zanello, P.; Vacca, A. *Inorg. Chem.* **1988**, *27*, 4429.

(6) Bianchini, C.; Meli, A.; Peruzzini, M.; Vizza, F. *Organometallics* **1990**, *9*, 2283.

(7) Bianchini, C.; Meli, A.; Peruzzini, M.; Vacca, A.; Vizza, F. *Organometallics* **1991**, *10*, 645. Bianchini, C.; Caulton, K. G.; Chardon, C.; Eisenstein, O.; Folting, K.; Johnson, T. J.; Meli, A.; Peruzzini, M.; Rauscher, D. J.; Streib, W. E.; Vizza, F. *J. Am. Chem. Soc.* **1991**, *113*, 5127.

(8) Barbaro, P.; Bianchini, C.; Meli, A.; Peruzzini, M.; Vacca, A.; Vizza, F. *Organometallics* **1991**, *10*, 2227.

(9) Janser, P.; Venanzi, L. M.; Bachechi, F. *J. Organomet. Chem.* **1985**, *296*, 229.

Scheme III. Thermal Behavior of 1 under Inert Atmosphere

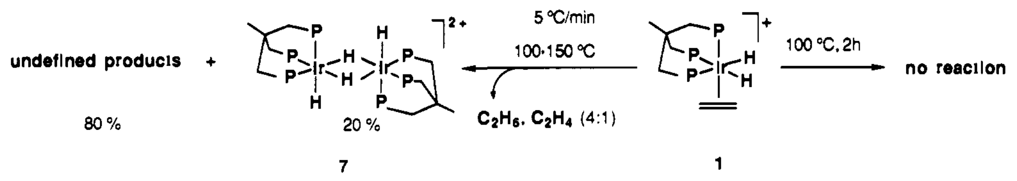

Scheme IV. Solid–Gas Reactions of 1 with CO or C_2H_4

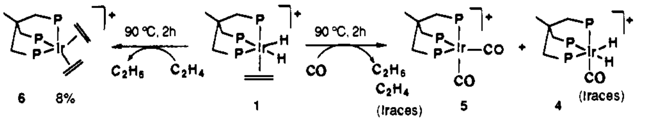

relevance as it suggests that *the unsaturated* $[(triphos)Ir(H)_2]^+$ *fragment formed by* C_2H_4 *elimination from 1 can dimerize in the solid state* (see forthcoming pages). In fact, were the formation of 7 due to dimerization in solution of $[(triphos)Ir(H)_2]^+$, this species would be first trapped by the coordinating solvent,[10] and then it would react with CO to give the known dihydride carbonyl 4 or, eventually, the dicarbonyl 5 (both reactions do occur under appropriate conditions, as shown in forthcoming pages).

Solid-Gas Reactions of 1 with CO or C_2H_4. Complex 1 reacts in the solid state with CO at 90 °C, almost quantitatively converting to the dicarbonyl 5 (^{31}P NMR, IR) (Scheme IV). In a typical experiment, CO is passed over crystals of 1 (200 mg) for 2 h by using the simple glass apparatus shown in the Experimental Section. Termination of the reaction is determined by the disappearance of the stretching band of the Ir–H bonds and the appearance of two $\nu(C{\equiv}O)$ bands at 2053 and 1954 cm^{-1}.

Quantitative determination of the gaseous phase during the reaction shows evolution of ethane (98%) and traces of ethylene (2%) (Scheme IV). Since the amount of ethylene evolved roughly corresponds to the amount of the dihydride carbonyl 4, one may hypothesize that CO can, although to a much lesser extent, displace the C_2H_4 ligand.

Evolution of ethane is observed also when crystals of 1 are reacted with C_2H_4 at 90 °C. In this case, however, the parent dihydride complex (200 mg, 2 h) transforms only partially (8%) into the bis(ethylene) complex 6.

Like the thermal decomposition under inert atmosphere as well as the solution chemistry of Scheme II, the evolution of ethane is consistent with a solid-state rearrangement of 1 to its hydride-migration product $[(triphos)Ir(H)(C_2H_5)]^+$ followed by reductive elimination of ethane. At this point, however, the presence of good ligands such as C_2H_4 or CO allows the $[(triphos)Ir]^+$ fragment to be stabilized.

Solid–Gas Reactions of 1 with H_2 and H_2/C_2H_4. With Dihydrogen. Crystals of 1 react with H_2 at 70 °C for 2 h, converting to a 1:1 mixture of the unsaturated fragment $[(triphos)Ir(H)_2]^+$ (8) and of the tetrahydride 7. The composition of the mixture can be determined (^{31}P NMR integration) by dissolving the crude product into THF-d_8 previously saturated with either CO or C_2H_4. In both cases, 50% of the starting "$(triphos)Ir(H)_2$" moiety of 1 remains trapped in a mononuclear complex (1 itself with C_2H_4, and the dihydride carbonyl 5 and the dicarbonyl 4 with CO) (Scheme V). In contrast, when the crude product of the reaction is dissolved in CD_2Cl_2, only the tetrahydride 7 is detected by ^{31}P NMR spectroscopy.

At this point one may argue that 1 reacts in the solid state with H_2 at 70 °C to give the unsaturated species 8, which might undergo two reactions at different rates in CO-unsaturated solution: the dimerization to 7 and the uptake of CO to give 4 and, successively, 5. This is not the case for the following reasons.

(i) The crude product of the reaction with H_2 reacts in the solid state with ethylene (70 °C, 2 h) to give an almost equimolecular mixture of 1 and 7 (NMR, CD_2Cl_2 solution). This indicates that the initial product contains a species, reasonably 8, which is able to pick up ethylene in the solid state, thus regenerating the starting dihydride ethylene complex. In a similar way, the reaction of the crude product in the solid state with CO (70 °C, 2 h) produces a mixture still containing 50% of 7 in addition to the dicarbonyl 5 and the dihydride carbonyl 4. Notably, 7 does not react in the solid state with CO.

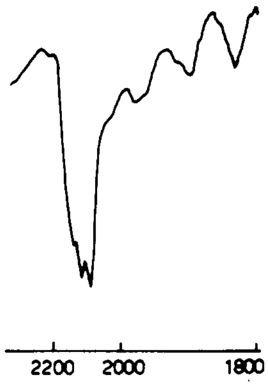

Figure 1. IR spectrum (Nujol mulls, KBr) in the hydride region of the products. The spectrum was obtained by reacting 1 with H_2 at 70 °C for 2 h.

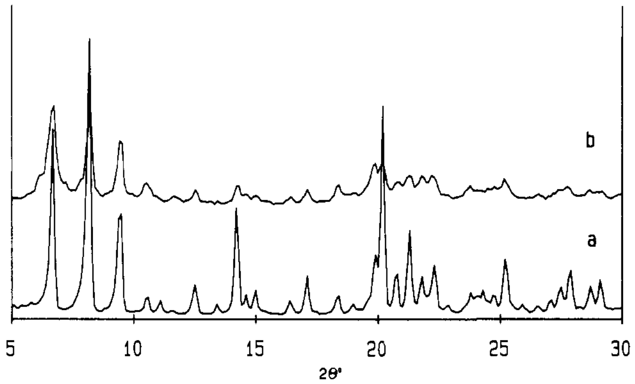

Figure 2. Powder X-ray spectra of 7 (a) and 1 after solid-state reaction with H_2 at 90 °C for 5 h (b).

(ii) The IR spectrum (Nujol mulls) of the product obtained from the solid–gas reaction with H_2 shows a broad band in the IR–H stretching region with three absorption maxima (Figure 1). Notably, the two higher energy absorptions (2124 and 2102 cm^{-1}) match well the values reported for a pure sample of 7 (2127 and 2104 cm^{-1}).[8] The third band at 2068 cm^{-1} may be, therefore, assigned to 8.

(iii) On increasing the reaction temperature, the percentage of the dimer increases (85% vs 50% after 2 h at 90 °C, Scheme V) at the expense of 8. Finally, complete conversion to 7 is achieved after 5 h at 90 °C. Strong experimental evidence for the solid-state dimerization reaction is provided by a comparison of the powder X-ray spectra shown in Figure 2 of the product obtained after 5 h at 90 °C (a) and of a pure sample of 7 (b). The integrated area of the three strong peaks in the range 2Θ = 5–10° in spectrum b accounts for 87% of the corresponding area of spectrum a; this suggests that only a limited loss of crystallinity has occurred during the reaction. A perusal of the two patterns shows that in spectrum b an additional shoulder in the peak at 6.1° is present, while the peaks at 11.1 and 25.8° are missing. However, the whole pattern strongly suggests that the two spectra

---

[10] Bianchini, C.; Caulton, K. G.; Folting, K.; Meli, A.; Peruzzini, M.; Polo, A.; Vizza, F. *J. Am. Chem. Soc.* **1992**, *114*, 7290.

Scheme V. Solid–Gas Reactions of 1 with H_2, H_2/C_2H_4, $H_2 + C_2H_4$, and $H_2 + CO$

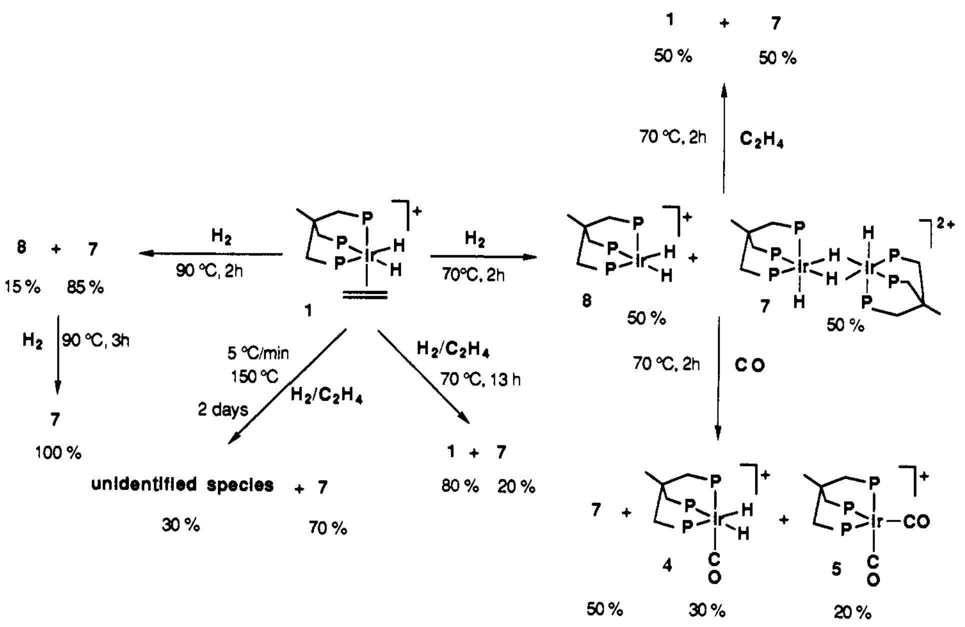

Scheme VI

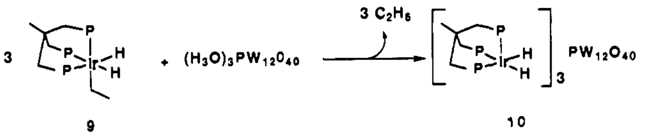

refer to isostructural compounds. The different relative peak intensities in the two spectra may be attributed to the possibility of preferential orientations of the crystallites in the two samples.

The assignment of the band at 2068 cm^{-1} and the ability of CO to trap **8** in the solid state is indirectly but substantially supported by the experiment illustrated in Scheme VI and inspired by previous works by Siedle.[1] In a series of elegant papers this author has shown that coordinatively unsaturated metal cations can be stabilized in interstitial sites in lattices formed by anionic metal oxide clusters such as $PW_{12}O_{40}^{3-}$. With this in mind, we have reacted the known dihydride ethyl complex $[(triphos)Ir(H)_2(C_2H_5)]$[8] (**9**) with $(H_3O)_3PW_{12}O_{40}$ (3:1 ratio) in acetone solution. With the addition of ethanol, white microcrystals of a compound analyzed as $[(triphos)Ir(H)_2]_3PW_{12}O_{40}\cdot(CH_3)_2CO$ (**10**) precipitate in quantitative yield. Interestingly, the IR spectrum of **10** (Nujol mulls) contains a unique band in the Ir–H stretching region at 2065 cm^{-1}. Most importantly, when **10** is allowed to react with a stoichiometric amount of CO in THF-d_8, the $^{31}P\{^1H\}$ NMR spectrum (sealed tube) shows the stoichiometric formation of the dihydride carbonyl complex **4**, whereas in DMF-d_7 under nitrogen only the dimer **7** forms. Compound **10** is quite stable in the solid state when heated at 150 °C. This indicates that the unsaturated metal cations are stabilized in the interstitial sites of the W oxide cluster, which, therefore, would prevent two **8** units from getting together.

In light of these results, one may reasonably conclude that by C_2H_4 elimination from **1** the unsaturated $[(triphos)Ir(H)_2]^+$ system is formed that has a relatively good stability in tetraphenylborate lattice at 70 °C, whereas at higher temperatures solid-state dimerization to the saturated tetrahydride **7** occurs.

With Dihydrogen/Ethylene. Having found that the unsaturated dihydride **8** is able to pick up C_2H_4 in the solid state, we decided to investigate the solid–gas reactions of **1** with a mixture of H_2 and C_2H_4. In keeping with the previous findings, the complex reacts with H_2/C_2H_4 in a tubular flow reactor (see Experimental Section) at 70 °C for 13 h, apparently with scarce modification as only 20% of **1** is converted to the dimer **7** (Scheme V). As expected, at higher temperatures and for a longer reaction time (5 °C/min up to 150 °C and then 2 days at 150 °C), the amount of the tetrahydride increases very much (70%). Under these reaction conditions, 30% of **1** is converted to a poorly soluble, unidentified species whose $^{31}P\{^1H\}$ NMR spectrum in DMF-d_7 appears as a broad singlet at −2.3 ppm. Notably, such a species is unreactive toward ethylene in both the solid state and solution.

Table I. Hydrogenation of Ethylene under Flow Conditions Catalyzed by **1** and **7**[a]

run	catalyst	T (°C)	rate[b] ($\times 10^2$)	E_a[c] (kJ/mol)	termination product[d]
1	**1**	70	3.5	4	**1** (80%), **7** (20%)
2	**1**	150	2.4		unidentified species[e] (30%), **7** (70%)
		70	0.2[f]	32	
3	**7**	150	3.5	31	**7** (100%)
		70	0.3		

[a] Reaction conditions: $W/F = 2.2 \times 10^{-3}$ g catalyst min mL^{-1}, $p(H_2) = 25.0$ kPa, $p(C_2H_4) = 5.0$ kPa, $p(Ar) = 71.3$ kPa. [b] Rate = moles C_2H_4 converted × mole Ir^{-1} × min^{-1}. [c] Measured in the range 40–70 °C, run 1; 50–150 °C, runs 2 and 3. [d] Characterized by solution NMR (CD_2Cl_2). [e] See text on p 11. [f] Catalyst recycled from run 2.

Since both reactions with H_2/C_2H_4 produce catalytic amounts of ethane, a detailed kinetic study of the solid–gas catalytic hydrogenation of ethylene assisted by **1** has been carried out.

Solid–Gas Catalytic Hydrogenation of Ethylene with 1 and 7. Hydrogenation reactions were carried out at atmospheric pressure in the temperature range from 50 to 150 °C. In a typical experiment, the following partial pressures and contact time were employed: 5.0 kPa C_2H_4, 25.0 kPa H_2, 71.3 kPa He, $W/F = 2.2 \times 10^{-3}$ g min mL^{-1}. Conversions were found to be proportional up to a contact time of 1.5×10^{-3} g min mL^{-1}. Steady-state activities obtained by using **1** and **7** as catalysts are reported in Table I. Notably, both **1** and **7** when used as catalyst precursors in the solid state show catalytic activity at temperatures as low as 70 °C (Table I, runs 1 and 3). However, at 70 °C the activity of **7** is about 10 times lower than that of **1**. This is not the case under homogeneous conditions, where both species are inactive at temperatures up to 150 °C (see below).

As a general trend, the activities observed showed no induction period, using both **1** and **7** as catalyst precursors. However, when **1** was employed as catalyst, on increasing linearly (5°/min) the reaction temperature a sudden increase of catalytic activity starting at about 80 °C was observed (Figure 3.1, curve a). The activity then dropped to a conversion of less than 2% at 150 °C (see also Table I, run 2). The partial deactivation of the catalyst appears to be irreversible since when the heating cycle was repeated the

Scheme VII. Catalysis Cycle for the Solid–Gas Hydrogenation of Eihylene Assisted by **1** at 60 °C

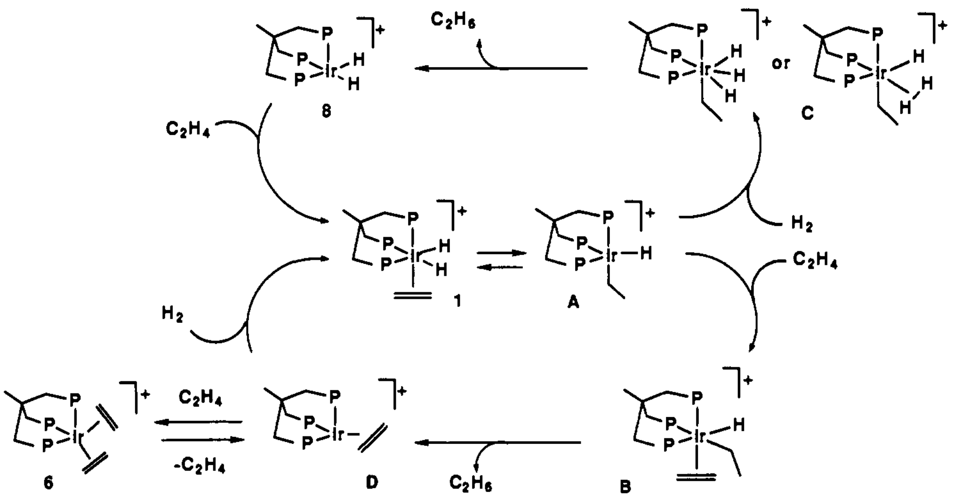

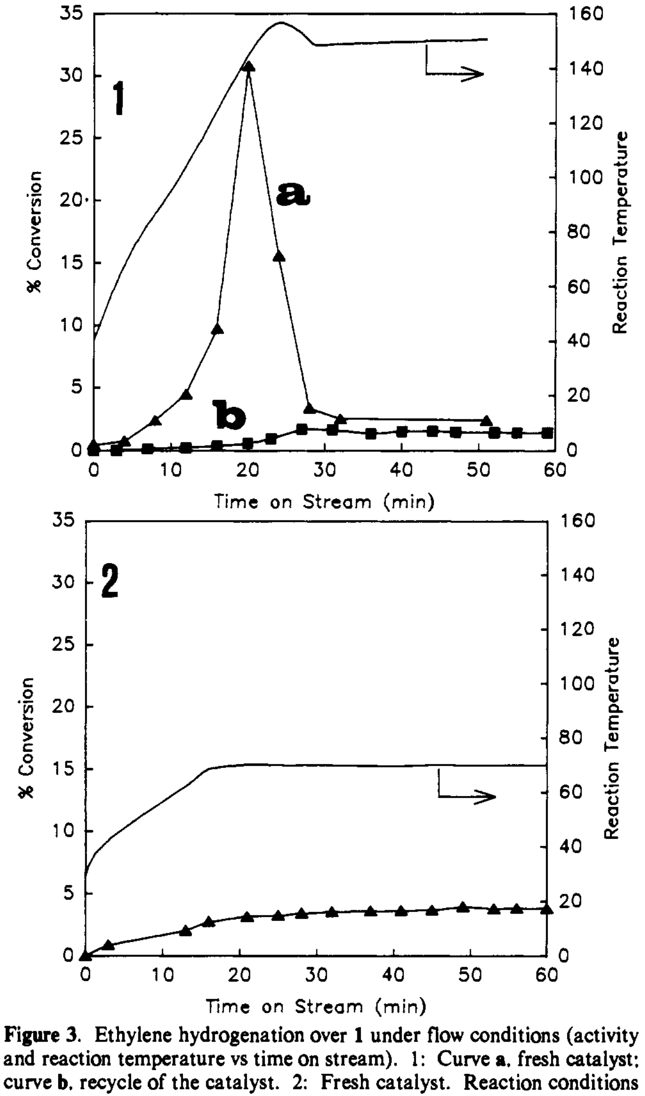

Figure 3. Ethylene hydrogenation over **1** under flow conditions (activity and reaction temperature vs time on stream). 1: Curve **a**, fresh catalyst; curve **b**, recycle of the catalyst. 2: Fresh catalyst. Reaction conditions are as reported in Table I, note a.

results reported in curve b of Figure 3.1 were obtained. Notably, the whole area of the peak reported in Figure 3.1 corresponds to a conversion of about 3 mol of C_2H_4/mol of **1**. Such a behavior was not observed for **7**, which behaves similarly to curve b of Figure 3.1.

As previously discussed, the deactivation of the catalyst **1** can be attributed to appreciable formation in the solid state of **7** and an unidentified species, which, in fact, were detected in about 7:3 ratio by ^{31}P NMR spectroscopy after the reaction depicted in Figure 3.1. Such a deactivation of the catalyst can be avoided as long as the reaction temperature is kept below 70 °C (Figure 3.2). However, even at this temperature some deactivation was observed on long reaction times. Thus, a maximum rate of 4.3×10^{-2} min^{-1} is found after 2 h, which then slowly decreases to a value of 3.5×10^{-2} min^{-1} after 15 h. An overall turnover number of 65 was measured for this reaction. At a reaction temperature of 60 °C, the steady-state conditions could be maintained for several days.

Dependence of the reaction rate on hydrogen and ethylene pressures was therefore measured at 60 °C, and the results are reported in Figure 4. A linear dependence on hydrogen pressure is observed, while for a slight inhibiting effect is observed at higher pressures of the reactants. A nonlinear regression of the data to a power-law expression of the form

$$r = kp(H_2)^a p(C_2H_4)^b$$

gives values of 0.51 ± 0.02 and 0.54 ± 0.02 for *a* and *b*, respectively. This suggests that traces of metal should not be responsible for the catalytic activity observed since typically reaction orders for ethylene hydrogenation catalyzed by metal surfaces are 1 in hydrogen and 0 in olefin.[11]

Incorporation of all of the above experimental evidence leads to the mechanism shown in Scheme VII for the solid–gas catalytic hydrogenation of ethylene. In accord with the chemistry of **1** illustrated in Schemes III–V, the dihydride ethylene complex can convert to the hydride ethyl derivative **A** via migration of H from metal to coordinated ethylene. Intramolecular migration of hydrogen atoms from metal to coordinated ligands occurring in the solid state have some precedent, particularly in the hydrocarbon chemistry of $[(Ph_3P)_2Ir(H)_2]_3PW_{12}O_{40}{}^2$ and in the thermal rearrangement of cobalt hydride alkynyls to cobalt vinylidenes.[2a]

Either C_2H_4 or H_2 can react with the electronically and coordinatively unsaturated system **A** to give $[(triphos)Ir(H)(C_2H_4)]^+$ (**B**) or $[(triphos)Ir(H)(C_2H_5)(H)_2]^+$ (**C**). The results presented in Schemes II and IV, particularly the observation that fragment **A** is stabilized by CO, yielding the hydride ethyl carbonyl **3**, support the occurrence of ligand addition to **A**. Addition of H_2 to **A** might give either a classical Ir(V) dihydride or a nonclassical Ir(III) dihydrogen metal complex.[12] The reductive elimination of ethane from species **B** and **C** then leads to the formation of **8** and **D**, respectively, which can readily restore the starting compound **1** by C_2H_4 or H_2 uptake. The presence of **8** in the catalytic cycle is substantiated by in situ IR spectra which show, besides

---

(11) Bond, G. C. *Catalysis by Metals*; Academic Press: New York, 1962.

(12) (a) Heinekey, D. M.; Millar, J. M.; Koetzle, T. F.; Payne, N. G.; Ziim, K. W. *J. Am. Chem. Soc.* **1990**, *112*, 909. (b) Mediati, M.; Tachibana, G. N.; Jensen, C. M. *Inorg. Chem.* **1990**, *29*, 5. (c) Gusev, D. G.; Bakhmutov, V. I.; Grushin, V. V.; Vol'pin, M. E. *Inorg. Chim. Acta* **1990**, *177*, 115.

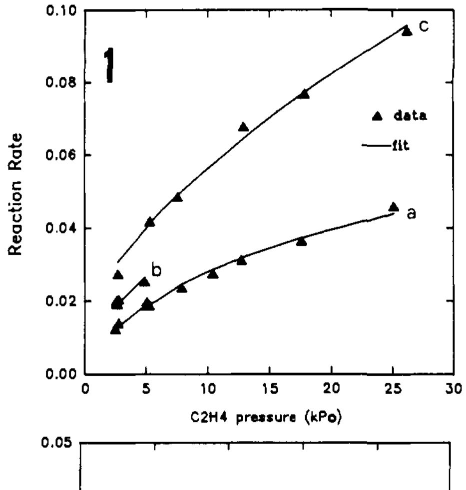

Figure 4. Ethylene hydrogenation at 60 °C over 1 under flow conditions. The graphs show reaction rate dependence on ethylene (**1**) (**a**, $p(H_2)$ = 12.5 kPa; **b**, $p(H_2)$ = 25 kPa; **c** $p(H_2)$ = 50 kPa) and hydrogen (**2**) (**a**, $p(C_2H_4)$ = 2.5 kPa; **b**, $p(C_2H_4)$ = 5 kPa) pressures.

the two predominant bands at 2110 and 2062 cm^{-1} due to **1**, the band at 2068 cm^{-1} attributable to **8**.

A side reaction that may poison the catalyst is the reaction of intermediate D with a second ethylene molecule to give **6**. Indeed, in nice accord with the slight inhibiting effect caused by increasing the pressure of C_2H_4, we have found that the reaction of solid **6** with H_2 is slower than that of solid **1** (at 70 °C for 2 h we note a 70% conversion of **6** to give almost equimolecular amounts of **8** and **7**).

However, as suggested by a reviewer, it is worth mentioning an alternative catalytic cycle. This involves the reductive elimination of ethane from species A to give the "naked" Ir(I) $[(triphos)Ir]^+$ fragment prior to interaction with either H_2 or C_2H_4. At present, we have no evidence for ethane elimination from **1** occurring in the solid state at 60 °C in the absence of H_2 or C_2H_4. As stated in preceding pages, the reaction occurs only above 100 °C. Detailed kinetic studies are in progress to further elucidate this mechanistic aspect.

A Comparison with Fluid Solution-Phase Systems. Under homogeneous conditions (THF 25 mL, substrate/catalyst 100, reaction time 3 h), neither **1** nor **7** is catalyst for the hydrogenation of ethylene up to 100 °C and 5 atm of H_2/C_2H_4. Actually, under these reaction conditions **1** rapidly transforms into **7**, as shown by NMR experiments. This finding suggests that site isolation, which is effective in the solid state, may be responsible for the different catalytic activity of **1** in the solid state and in solution. At 150 °C, **7** is still inactive, whereas **1** proves to be an effective catalyst precursor. Interestingly, however, the termination product of the reaction is the known trihydride $[(triphos)Ir(H)_3]^9$ (**11**), which is recovered in quantitative yield at the end of the reaction when all ethylene has been consumed. This result is quite surprising as the reaction starts with a cationic complex having an even number of hydride ligands and ends to give a neutral species with an odd number of hydrides. Such a transformation formally

Scheme VIII

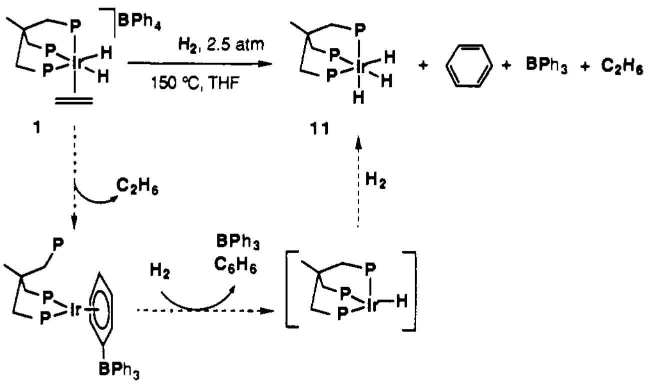

requires a heterolytic splitting of dihydrogen.[13] Indeed, we have found that the reaction of **1** in THF at 150 °C with H_2 (2.5 atm) stoichiometrically gives the trihydride **11**, ethane, benzene, and BPh_3. These results clearly indicate the participation of the BPh_4^- anion in the splitting reaction assisted by iridium:

$$BPh_4^- + H_2 \xrightarrow{Ir} BPh_3 + C_6H_6 + H^-$$

A reasonable mechanism for the **1** → **11** conversion is shown in Scheme VIII. This involves the activation of tetraphenylborate by the unsaturated $[(triphos)Ir]^+$ fragment, which forms after C_2H_6 elimination. Although we have not been able to detect any product containing tetraphenylborate coordinated to iridium, it is noteworthy that a related complex (namely, $[(\eta^2\text{-triphos})Rh(\eta^6\text{-PhBPh}_3)]$) has recently been obtained by Caulton and Thaler by interaction of "naked" $[(triphos)Rh]^+$ with BPh_4^-.[14] An iridium complex of this type may react with H_2 to give benzene, BPh_3, and the 16-electron fragment, which is appropriate to form **11** via the oxidative addition of H_2.

Actually, **11** is an effective catalyst for the hydrogenation of ethylene to ethane, even at lower temperatures (100 °C), thus suggesting that the homogeneous reaction assisted by **1** proceeds via conversion of the latter complex to **11**.

Conclusions

The present study has shown that solid-state organometallic reactions can be carried out in both stoichiometric and catalytic ways with no need of metal oxide clusters to stabilize unsaturated species. As compared to analogous reactions with metal oxide clusters,[2] the use of the tetraphenylborate salts of tripodal polyphosphine complexes may simplify the reactions as well as the identification of the products. In particular, through these reactions there is hope of increasing the molecular-level understanding of heterogeneous reactions, which is much less advanced than that at the homogeneous level.[15] On the other hand, it remains to ascertain whether other counteranions are as effective as BPh_4^- in assisting solid–gas reactions. Indeed, the BPh_4^- anions provide an extensive hydrophobic region through which small organic molecules can easily diffuse.[2b]

The heterogeneous chemistry that occurs at the iridium center in the unsaturated system $[(triphos)Ir(H)_2]^+$, particularly as regards the hydrogenation of ethylene, diverges from that observed in solution in which dimerization to the inactive tetrahydride **7** is a very fast process.

Of particular relevance is the dimerization of **8** to **7** occurring in the solid-state which is controlled by the temperature. To the best of our knowledge, no reaction of this type has been reported so far in inorganic chemistry,[16] whereas solid-state bimolecular

---

[13] Bianchini, C.; Meli, A. *Inorg. Chem.* **1987**, *26*, 4268. For a review article, see: James, B. R. In *Comprehensive Organometallic Chemistry*; Wilkinson, G., Stone, F. G. A., Abel, E. W., Eds.; Pergamon: Oxford, England, 1982; Vol. 8, p 285.

[14] Thaler, E. G.; Caulton, K. G. *Organometallics* **1990**, *9*, 1871.

[15] Parshall, G. W. *Homogeneous Catalysis*; Wiley: New York, 1980. Gates, B. C.; Schuit, G. C. A. *Chemistry of Catalytic Processes*; McGraw-Hill: New York, 1979.

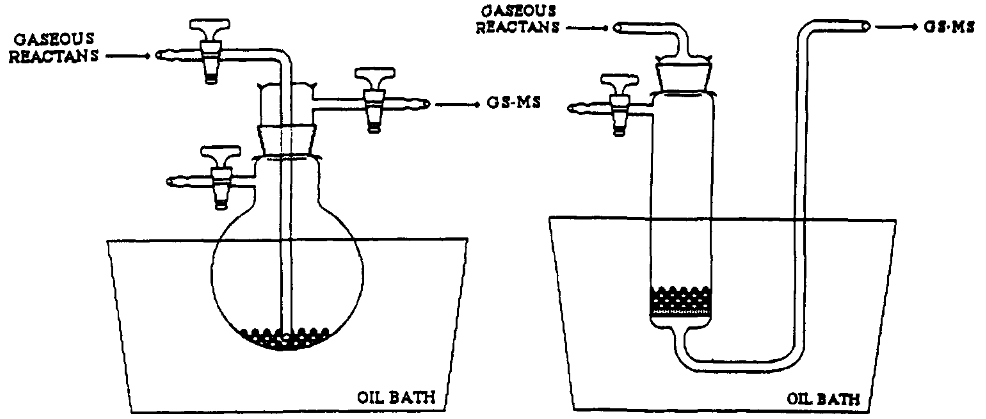

Figure 5. Apparatus used to carry out some solid–gas reactions.

reactions are well known in organic chemistry.[17]

Finally, it is worth pointing out the ability of the "(triphos)Ir" system to coordinate in the solid state C_2H_4, H_2 and CO, namely the three ingredients of hydroformylation reactions. Accordingly, our approach may open a new way to accomplish the solid–gas hydroformylation reactions which are presently attracting so much interest.

Experimental Section

Tetrahydrofuran (THF) was purified under argon just prior to use by distillation over $LiAlH_4$. Hydrated $(H_3O)_3PW_{12}O_{40}$ was purchased from Alfa Products. All the other solvents and chemicals were reagent grade and, unless otherwise stated, were used as received from commercial suppliers. Deuterated solvents for NMR measurements (Janssen) were dried over molecular sieves. Infrared spectra were recorded on a Perkin-Elmer 1600 Series FTIR spectrophotometer using samples mulled in Nujol between KBr plates. Proton NMR spectra were recorded at 299.945 MHz on a Varian VXR 300 spectrometer or at 200.131 MHz on a Bruker 200-ACP spectrometer. Peak positions are relative to tetramethylsilane as external reference. $^{31}P\{^1H\}$ NMR spectra were recorded on the same instruments operating at 121.421 and 81.015 MHz, respectively. Chemical shifts are relative to external 85% H_3PO_4, with downfield values reported as positive. High pressure experiments were performed using a Parr Model 4564 stainless steel minireactor (vol 100 mL) with a magnetic drive stirrer and an elec mantle as heating source. Analysis of the products of the catalytic reactions was carried out on a Shimadzu GC-8A gas chromatograph fitted with a thermal conductivity detector and with a 10-ft 100/120 Carbosieve-SII stainless steel column (Supelco Inc.). Quantification was achieved with a Shimadzu C-R6A Chromatopac coupled with the chromatograph, operating with an automatic correct area normalization method. GC-MS spectra were collected with a Shimadzu QP-2000 fitted with the 30-m (i.d. 0.25 mm) capillary column Supelco SPB-1. Powder X-ray spectra were obtained on a Siemens D500 instrument using a Ni-filtered CuKα radiation. The TPDE experiments were carried out in the same apparatus used for the catalytic reactions in flow conditions (see below).

Solid-State Reactions. Reactions of **1** with gases were carried out either in the simple glass apparatus shown in Figure 5 or in the tubular flow reactor described below.

After the complex (200 mg) was placed inside, the glass container was evacuated to $<10^{-4}$ Torr and then immersed in an oil bath maintained at the experimental temperature. The reaction vessel was carefully backfilled with a steady stream of the appropriate gaseous substrate for 2 h.

Termination of every reaction can be determined by IR (KBr) spectroscopy on samples withdrawn periodically.

Catalytic Reactions in Flow Conditions. Dynamic hydrogenation runs were carried out in a stainless steel tubular flow reactor operating in differential conditions at atmospheric pressure. Blank experiments showed negligible conversions in the reaction conditions employed. Typically 80 mg of catalyst was loaded between two layers of granular quartz, which acts as preheater. The reactor was then deareated in a flow of He and heated to the desired temperature, and then the reactants (H_2 and C_2H_4) were admitted. The desired partial pressures were adjusted to constant flow with He as diluent. The absence of diffusional effects was verified. The reaction temperature was measured by means of a thermocouple located in the catalyst bed. The analyses were carried out on an on-line Varian 3400 gas chromatograph equipped with a flame ionization detector. Separation of the products was achieved on a Porapak Q column. IR spectra were taken on a Perkin-Elmer 983 spectrophotometer equipped with a Perkin-Elmer 3600 Data Station. For the in situ measurements a stainless steel IR cell constructed according to ref 18 was employed. The catalyst precursor was deposited on the surface of the KBr windows from an undecane suspension.

Solution Syntheses. All reactions and manipulations were routinely performed under a dry argon or nitrogen atmosphere. The solid compounds were collected on sintered-glass frits and washed with ethanol and petroleum ether (bp 50–70 °C) before being dried in a stream of argon. Compounds **1**–**7**[8], **9**[8], and **11**[9] were prepared according to literature methods.

Synthesis of $[(triphos)Ir(H)_2]_3PW_{12}O_{40}\cdot(CH_3)_2CO$ (10). Solid $(H_3O)_3PW_{12}O_{40}$ (0.51 g, 0.18 mmol) was added with stirring to a solution of **9** (0.60 g, 0.51 mmol) in acetone (50 mL) at room temperature under argon. Immediate evolution of ethane was observed. After addition of ethanol (50 mL) and concentration of the reaction mixture under a slow stream of argon, off-white microcrystals of **10** precipitated which were collected by filtration and washed with ethanol and *n*-pentane, yield 98%. IR (Nujol mulls, KBr): 2065 cm^{-1}, ν(Ir—H); 1658 cm^{-1}, ν(C═O) (this band may indicate the presence of coordinated acetone).[2] $^{31}P\{^1H\}$ NMR (DMF-d_7, 81.015 MHz): singlet at −19.8 ppm, A_3 spin system of **7**; singlet at −15 ppm, $PW_{12}O_{40}{}^{3-}$ cluster. ^1H NMR (200.131 MHz): septet at −13.3 ppm, J(HP) = 17.0 Hz, δ(Ir–H). $^{31}P\{^1H\}$ NMR (CD_3COCD_3 + CO, 81.015 MHz): AM_2 spin system, δP_A −11.5, δP_M −21.7 ppm, $J(P_AP_M)$ = 27.1 Hz. ^1H NMR (200.131 MHz): −10.18 ppm, δ(Ir–H), $J(HP_{trans})$ = ca. 110 Hz. Anal. Calcd for $C_{126}H_{129}Ir_3O_{41}P_{10}W_{12}$: C, 28.0; H, 2.5; Ir, 10.8; P, 5.7; W, 40.9. Found: C, 27.7; H, 2.4; Ir, 10.9; P, 5.8; W, 41.0.

Synthesis of $[(triphos)Ir(H)_3]$ (11). Air was evacuated from a 100-mL stainless steel autoclave containing **1** (0.20 g, 0.17 mmol), and then the solvent (25 mL of THF plus 0.5 mmol of toluene as internal standard) was introduced by suction. Hydrogen was added up to a pressure of 2.5 atm, and the autoclave was heated at 150 °C. After 2 h the reaction was stopped and the reaction mixture cooled at room temperature. GC-MS analysis revealed the stoichiometric formation of benzene and ethane. After distillation of the solvent at reduced pressure, a white crystalline sublimate was obtained at 70 °C (0.5 Torr). This air-sensitive product was identified by elemental analysis and infrared spectroscopy as triphenyboron.[19] The remaining product was shown to be pure $[(triphos)Ir(H)_3]$ (NMR, IR).[9]

Acknowledgment. Thanks are due to Prof. P. Frediani (University of Florence) for some homogeneous catalytic reactions and to Prof. G. Tauzher (University of Trieste) for helpful discussions. "Progetto Finalizzato Chimica Fine II" CNR, Rome, is acknowledged for financial support.

---

(16) Le May, H. E., Jr. In *Comprehensive Coordination Chemistry*; Wilkinson, G., Ed.; Pergamon Press: New York, 1986; Vol. 7, p 463.

(17) *Organic Solid State Chemistry*; Desiraju, G. R., Ed.; Elsevier: Amsterdam, 1987. Toda, F.; Yagi, M.; Kiyoshige, K. *J. Chem. Soc., Chem. Commun.* **1988**, 958.

(18) Hicks, R. F.; Kellner, C. S.; Savatsky, B. J.; Hecker, W. C.; Bell, A. T. *J. Catal.* **1981**, *71*, 216.

(19) Sharp, D. W.; Sheppard, N. *J. Chem. Soc.* **1957**, 674.